iVES OENO One vine & wine

DOI: https://doi.org/10.20870/oeno-one.2023.57.3.7216

OPEN ACCESS

ORIGINAL RESEARCH ARTICLE

A mobile device to investigate the response of grapevine berries to heat stress

Kai Konstantin Heilemann[1]*, Manfred Stoll[1], Marco Hofmann[1] and Matthias Friedel[1]

[1] Hochschule Geisenheim University, Department of General and Organic Viticulture, Von-Lade-Strasse 1, 65366 Geisenheim

*correspondence: kaikonstantin.heilemann@hs-gm.de

Associate editor: Eric Gomes

Received: 16 March 2023

Accepted: 20 July 2023

Published: 19 September 2023

ABSTRACT

Reproducibly comparing the heat stress response of grapevine berries from different cultivars in the field is often limited by weather conditions during the growing season. This work presents a mobile heating device capable of controlled heat-stress induction on grapevine berries. The heater consisted of six 150 W infrared lamps mounted in a profile frame. The heating power of the lamps could be set individually by a control unit consisting of a single board computer and six temperature sensors positioned as desired. The heat energy applied to individual berries within a cluster decreases by the squared distance to the heat source, enabling the establishment of temperature profiles within individual clusters. Infrared thermography of the fruit surface and measurements conducted with a thermocouple inserted at the epidermis level showed comparable temperatures. Berries treated with high temperatures were sampled according to their visual appearance (i.e., sunburn symptoms). Only symptomatic berries showed a significant increase in electrolyte leakage, indicating cell damage. In a field experiment, the induction of sunburn necrosis symptoms with the presented device was used to predict a Lethal Dose (LD_{50}) for sunburn necrosis symptoms of the *Vitis vinifera* L. cultivars Bacchus and Silvaner. The LD_{50} of Bacchus, known as a heat-sensitive cultivar, was about 3.2 °C lower than that of Silvaner. The presented device offers possibilities for a wide range of applications and the induction of precise temperature dynamics in the context of heat stress on fleshy fruit.

KEYWORDS: *Vitis vinifera*, heat stress, fruit surface temperature, sunburn, infrared thermography

INTRODUCTION

Heatwaves and extreme high-temperature events are expected to occur more frequently in the context of climate change (IPCC *et al.*, 2021; Meehl and Tebaldi, 2004). Therefore, threshold temperatures for heat damage on grapevine berries are more likely to be met, posing a challenge for grape growers and breeders. Heat stress affects plants on all levels, triggering complex responses that vary among and within species (Wahid *et al*., 2007). Grape berries ripening under elevated temperatures were found to have lower acidity, higher pH, higher sugar levels and lower anthocyanin content, potentially decreasing wine quality (Venios *et al*., 2020). Direct damage to berries, such as sunburn browning or sunburn necrosis (SN), may impact crop value and reduce yield and fruit quality (Gambetta *et al*., 2021).

Under high light conditions and heat stress, the excessive formation of reactive oxygen species (ROS) leads to damage to the photosynthetic apparatus, degradation of chlorophyll and a loss of cell wall integrity, ultimately causing cell damage and necrosis (Gill and Tuteja, 2010). The loss of cell wall integrity under severe heat stress exposes polyphenols to polyphenol oxidases, which causes the typical reddish-to-brown colour of the skin and flesh of SN berries (Gambetta *et al*., 2021).

The formation of high amounts of ROS is known to activate K^+-selective channels, leading to K^+-efflux from the cells, which can be measured as electrolyte leakage. Excessive leakage of K^+ from the cells triggers the onset of programmed cell death but may also trigger adaptation processes, leading to enhanced stress resilience (Demidchik *et al*., 2014).

To prevent damage to proteins, nucleic acids and the photosynthetic apparatus under high light and heat conditions, plants have evolved a wide array of protective mechanisms, possessing the ability to quench ROS (Gambetta *et al*., 2021). Chlorophyll, carotenoids and phenolic compounds are pigments known to inhibit ROS formation and act as scavengers, reducing ROS present in the apoplast (Munné-Bosch and Vincent, 2019). The importance of these mechanisms in ecophysiological interactions has sparked a great deal of research interest by plant physiologists as well as breeders regarding climate change.

During heatwaves, ambient temperatures are significantly higher compared to the normal temperatures for the region and season, while global radiation levels may remain unaffected as they cannot exceed the usual radiation of cloud-free weather conditions. Hence, many research efforts have focused on separating light and temperature effects to understand plant behaviour under such circumstances better (Spayd *et al*., 2002; Hulands *et al*., 2014). While experiments on potted plants in controlled environments seem ideal for investigating heat damage caused by elevated air temperatures, their results are often not reproducible under field conditions. This is especially true for permanent cultures, where plant and root size are limited by pot size and root temperatures may reach levels rarely found in the field. However, manipulating berry temperatures in the field is difficult to achieve. Tarara *et al*. (2000) heated or cooled clusters stationary in the field by forced convection with air conditioners mounted on insulated enclosures to separate light and temperature effects. An adapted system was used to study developmental and metabolic changes under elevated temperatures (Gouot *et al*., 2019). Due to the usage of fans, air blown on clusters may alter berry transpiration and consequently restrict some areas of application. A stationary approach to elevated temperatures in the field was introduced by Sadras *et al*. (2012). A panel system was used to elevate temperatures at the canopy level by ~ 2 °C. Since the temperature increase in such a system relies on ambient conditions, this method may probably not be sufficient to induce severe heat stress under high temperatures and, therefore, restrict several research fields like sunburn in early or late periods of the vegetation when ambient temperatures are relatively low.

Berry temperatures in such experiments are often measured by using thermocouples. This technique is restricted to single-point measurements, thus limiting the ability to record berry hotspot temperatures or temperature distributions

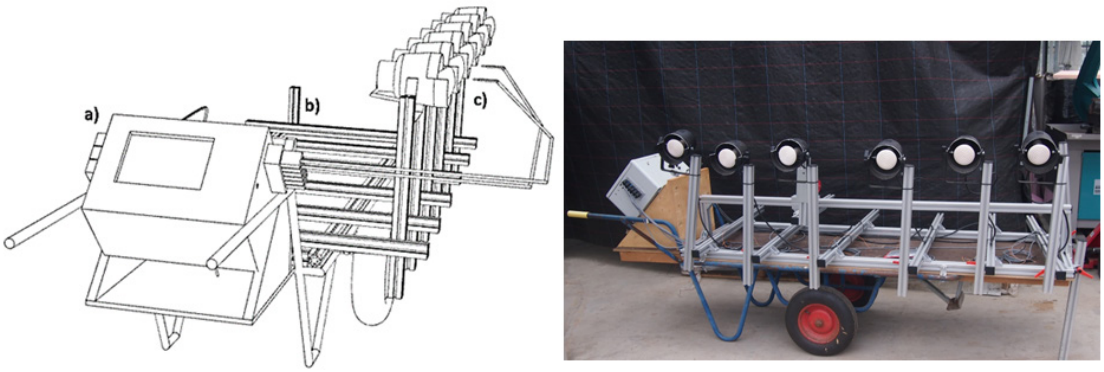

FIGURE 1. The moveable heating device.

Left: Schematic drawing of the moveable heating device. a) Controlling unit with touchscreen, including power and sensor connections. b) Modular profile system to position heating units in three directions. c) Six heating units consisting of spots, lamps, upper visor and temperature sensor. Right: Digital image of the moveable heating device.

within a cluster. Thermal imaging has proven to be a fast, precise and non-invasive technology to determine tissue surface temperature and offers the opportunity to record high amounts of single-berry surface temperatures (Stoll and Jones, 2007). Schrader *et al*. (2001) demonstrated the correlation of fruit surface temperatures with different sunburn symptoms, making infrared thermography a promising method to determine the influence of temperature on sunburn. Using this method, Ranjan *et al*. (2020) developed a stationary monitoring device that measures fruit surface temperature of exposed apple fruit in canopies, providing real-time data.

In this paper, we present a simple method to induce heat stress on grapevine berries based on using infrared radiant heaters to control the temperature of berries in field-grown vines without modifying photosynthetic active radiation or creating artificial air convection. The system is moveable within vineyards of common practice. The aim was to manipulate berry temperature dynamics in a reproducible manner, which will offer opportunities to gain knowledge in understanding heat stress, threshold temperatures and the phenomenon of sunburn in grapevine.

MATERIALS AND METHODS

1. Structure of the heating unit

Six 150 W infrared radiant heaters (Westfalia, Hagen, GER) were used as heating sources. The lamps are conical in shape with a flat front surface of 4.5 cm radius. Its emissivity was assumed to be 0.90, as reported by PEWA (2009) for white lacquered ceramic. A 4 cm modular profile system (Bosch Rexroth, Lohr am Main, GER) was set up to support radiators on a two-wheeled long barrow of 3 m length (Figure 1). Lamps were mounted in spots (230 V, Par28, EUROLITE, Waldbüttelbrunn, GER) with a 5 cm cut-out on the upper half of the visor to avoid shading when clusters are heated in sunlight. The profile system allowed adjustments in three dimensions for each heating unit to be positioned individually in front of the cluster. Six PT1000 temperature sensors (Heraeus Nexensos, Hanau, GER, accuracy ± 0.55 K at 50 °C) provide the ambient temperature (T_A) to the central temperature control unit, which controls the temperature by comparing T_A with the desired temperature setpoint (T_S) and regulates the power of the infrared radiant heaters (Figure 2). During measurements, the temperature sensors were positioned in the centre of the cluster to control the desired temperature profile.

2. Structure and functionality of the control unit

A single-board computer (model: Raspberry Pi® 3, Raspberry Pi® foundation, Cambridge, UK) with a LINUX operation system was used together with a power supply, power stage with phase control modulator, powering the infrared heater and a 10.1" Touch Screen (model: LCD 10 V2, Joy-IT, Neukirchen-Vluyn, GER) on top for manual operation. As shown in Figure 2, the central unit can control six channels simultaneously. The temperature controller uses a proportional-integral-derivate control algorithm, which lowers the power of the lamp before reaching T_S and, therefore, avoids exceeding T_S. The six-channel temperature control is realized by customized Python™ software. The temperature sensors are read by high-precision analog-to-digital converters, which provide the digital value to the single-board computer via Serial Peripheral Interface (SPI) every second. The T_S values are delivered either by manual input via touchscreen or by an input file in automatic mode, which offers the possibility to apply temperature profiles over an adjustable period.

T_S (°C), T_A (°C), emitter power (%) and power-on time (s) are displayed on a touchscreen in real-time for each heating unit. Data records can be started manually and saved to an output file for each of the above-mentioned parameters. The data is stored as csv files within the single-board computer and is accessible via ethernet cable from board-computer to PC by using standard File-Transfer-Protocol (FTP).

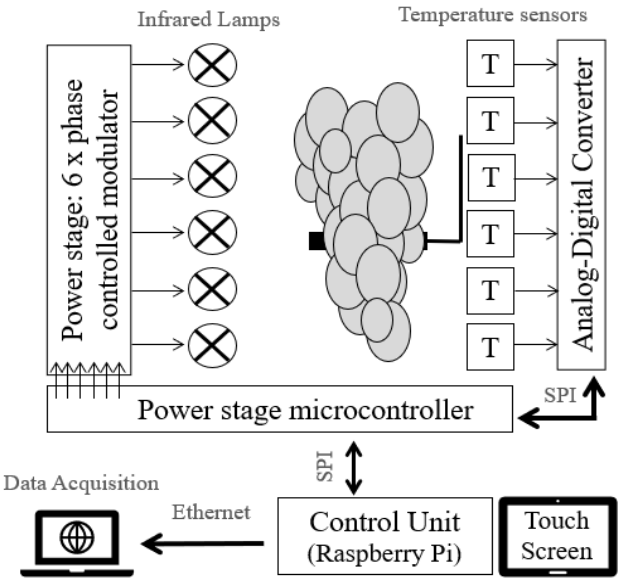

FIGURE 2. Block diagram of the hardware of the heating device.

The actual temperature of the temperature sensors is provided via the Serial Peripheral Interface (SPI) to the control unit. The control unit regulates the power of each infrared lamp by comparing the actual temperature given by the temperature sensor with an individually pre-set temperature using a power stage microcontroller and an Analog-Digital Converter.

2.1. Influence of the distance of a berry sample to the lamp on maximum fruit surface temperature and received radiation

A single detached berry (cv. Thompson seedless) was placed centrally along the longitudinal axis in front of one heating unit. While the lamp was running on maximum power (150 W), the berry was placed at distances (*h*) of 7, 10, 15 and 20 cm to the lamp, starting with the largest distance and gradually decreasing at time intervals of 30 minutes. A thermal image of the berry was taken to measure the fruit surface temperature of the hotspot of the

berry (FST_m), which was approximated by visually selecting an area of 1 cm² on the berry front surface. The ΔFST was calculated as the difference of the initial berry FST_m and the corresponding FST_m.

The influence of the distance between the berry and the lamp on the radiant flux intercepted by the berry surface $\varphi_{e\text{-}b}$ was calculated as

(1) $$\varphi_{e-b} = F_{l-b}\,\varphi_{e-l}$$

where $\varphi_{e\text{-}l}$ is the radiant flux leaving the front radiating surface of the lamp, $F_{l\text{-}b}$ is the view factor of the lamp to the berry and $\varphi_{e\text{-}b}$ is the resulting radiant flux from the lamp received by the berry surface. The view factor $F_{l\text{-}b}$ describes the dependency of the radiant energy exchange between the berry and the lamp on their geometric arrangement (orientation, size and separation distance) (Modest, 2003). $F_{l\text{-}b}$ was calculated assuming the lamp is a grey, diffuse emitter. The incident radiation hits the spherical berry over its entire front hemisphere. The radiation emitted by the lamp was assumed to originate from a round cross-section of the lamp. Both objects can be seen to be coaxial, parallel disks with a given radius lamp (r_l) and radius berry (r_b). For this geometry, the following solution to calculate the view factor was outlined by (Modest, 2003):

(2.1) $$F_{l-b} = \frac{r_b}{r_l}\,(X - \sqrt{X^2 - 1})$$

with X defined as

(2.2) $$X = \frac{h^2 + {r_l}^2 + {r_b}^2}{2 r_l r_b}$$

where h is the distance between the parallel disks representing the lamp and the berry. The radiant flux of the lamp ($\varphi_{e\text{-}l}$) was calculated as

(2.3) $$\varphi_{e-l} = \varepsilon\,\sigma\,A_l\,{T_l}^4$$

where ε is the emissivity of the lamp (0.90), σ is the Stefan–Boltzmann constant (5.67×10^{-8} W·m^{-2}·K^{-4}), A_l is the surface of the front of the lamp (0.0063 m²) and T_l (601.9 K) is the surface temperature of the lamp. The latter was measured as the mean surface temperature of the entire front of the lamp, 40 minutes after it was switched on. The resulting $\varphi_{e\text{-}l}$ was 42.58 W.

The irradiance received by the berry (E_b) is calculated as

(3) $$E_b = \frac{\varphi_{e-b}}{A_b}$$

where $\varphi_{e\text{-}b}$ was calculated as described in Eq. (1) and A_b is the surface of a disk with the radius of the berry (0.95 cm).

Thermography of berries was performed with a 1.2 MP infrared thermal imaging camera (model: InfReC R500EX, Fa. Nippon Avionics, Yokohama, Japan) set to 0.98 emissivity. Analysis of FST_m was conducted with InfReC Analyzer NS9500 Standard (Version 5.0C, Fa. Nippon Avionics, Yokohama, Japan). The software calculates the mean FST based on a manually selected area of pixels in a picture.

2.2. Comparison of thermocouple sensor measurements and thermography

A detached cluster of cv. Thompson seedless was set up in front of the heating unit with the nearest berry skin and a temperature-sensor beneath being at 7 cm distance to the nearest outline of the centre of the lamp. To provide the actual temperature of the berry cuticula, a copper-constantan thermocouple (Type T) was inserted from the backside of the berries to the side facing the heater, with the tip positioned underneath the epidermis. Temperature data was logged with a CR300 Datalogger (Campbell Scientific, Logan, USA) in 2-second intervals. The initially measured T_A was 22.5 °C, and T_S was set to 28 °C. Thermograms of the cluster were taken in 120-second intervals. The FST_m was measured with thermal images exclusively in the area in which the thermocouples were located (approx. 5 mm²). For comparison with thermography, the thermocouple temperature readings within a 20 s interval around thermogram acquisition were averaged.

2.3. Electrolyte leakage Measurements

The electrolyte leakage experiment was conducted at the Irrigated Agriculture Research and Extension Center at Prosser, Washington, USA on 18 June 2022. Three clusters of a Riesling vine (clone FPS 09, own-rooted), grown under full irrigation, were heated to a target temperature of 48 °C for 25 min with sunlight excluded. A thermal image and a digital image were taken immediately after the lamps were turned off. Before sampling, ten berries per cluster were annotated on the thermal image. Single berries were detached individually by cutting the pedicel from the rachis and stored in previously labelled falcon tubes corresponding to the annotation on the thermal image. Likewise, ten berries on three control clusters that were not heated were sampled in the same way. The stem of each berry was dipped in liquid but not steaming wax. The berries were rinsed with distilled water in a petri dish, and 5 ml of distilled water was added to the tube. The electrical conductivity (EC) of each sample was measured using a conductivity meter (model S400, Fa. Mettler-Toledo, Columbus, USA) before adding the berry (EC1), after the berry was added and the tube was carefully inverted (EC2) and after the sample was stored at - 60 °C for 4 hours followed by 12 hours at room temperature (EC3). The water temperature of each measurement was at 22 °C. The relative Electrolyte Leakage (REL) was calculated as follows:

(4) $$REL = \frac{EC2-EC1}{EC3} * 100$$

2.4. Comparison of cv. Bacchus and Silvaner for sunburn susceptibility

The experiment was carried out in a vineyard of the Hochschule Geisenheim University in Germany in 2021. Eight-year-old *Vitis vinifera* L. cvs. Bacchus and Silvaner were used for the heating experiments. These cultivars were chosen as they represent a very sunburn-susceptible (cv. Bacchus) and a relatively heat-tolerant cultivar (cv. Silvaner) and have been used for sunburn experiments in the past (Kolb *et al*., 2006).

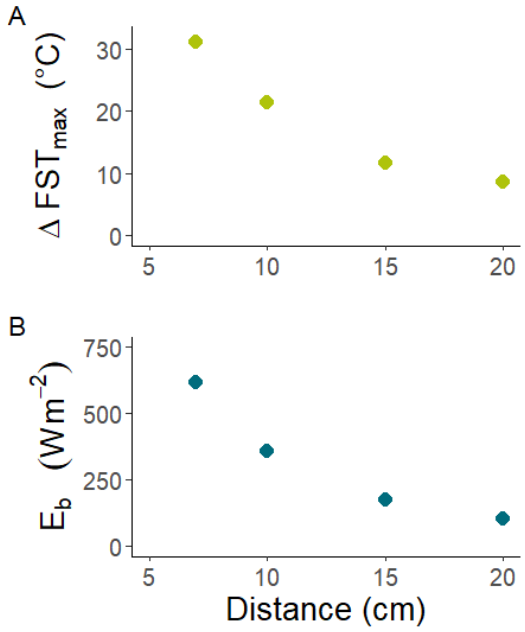

FIGURE 3. Influence of the distance of the berry to the heat source on berry temperature and received radiation.

A: Maximum temperature of the hotspot of the berry with distances of the lamp set to 20, 15, 10 and 7 cm, respectively. B: Calculated values of the radiant flux density (E_b) received by the berry surface for the above-mentioned distances.

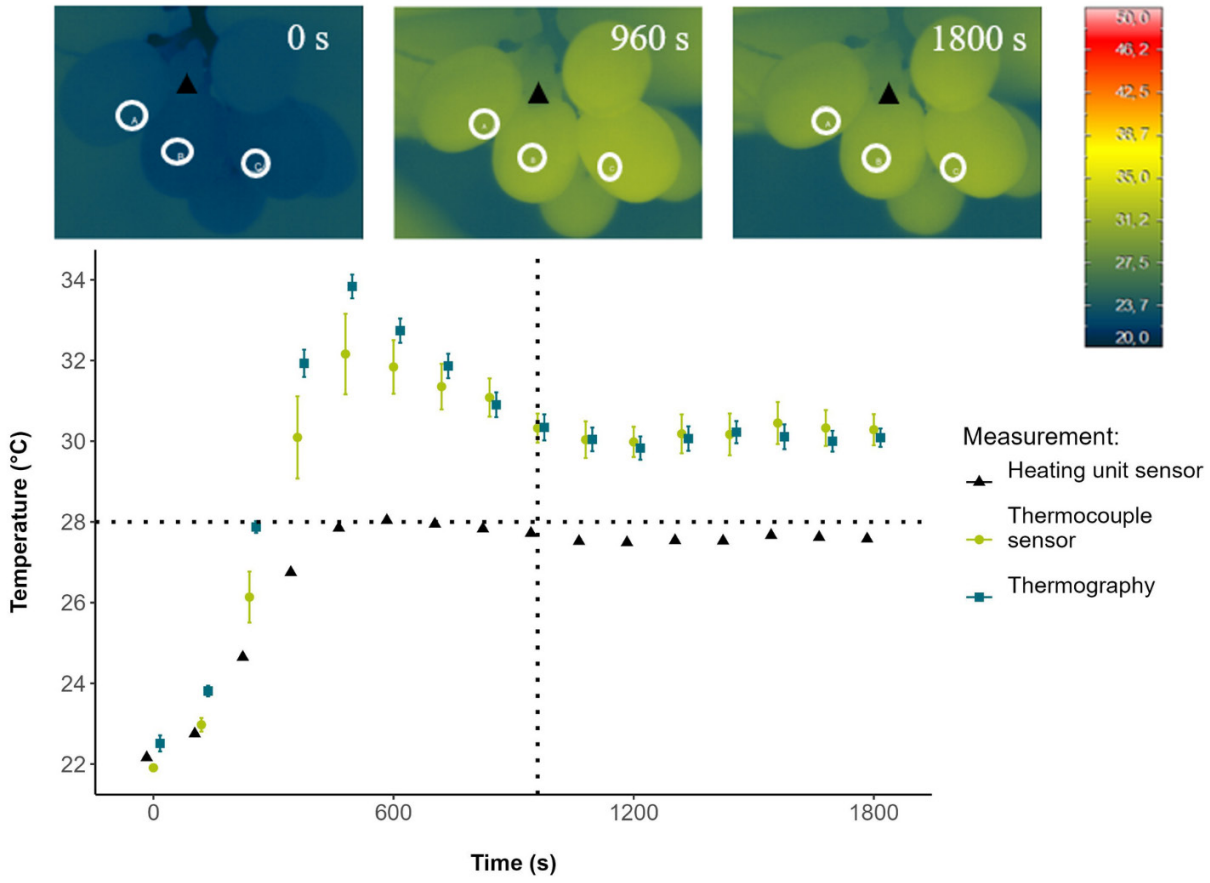

FIGURE 4. Comparison of thermocouple measurements and thermography.

Temperature measurements of the area of the fruit surface of three berries, as indicated by the white circles, heated to a target temperature of 28 °C. Thermal images were taken in two-minute intervals and compared to thermocouple measurements. Three thermograms of the detached cluster at the start, at 960 s (vertical dotted line) and at the end of the heating experiment (1800 s) are displayed. The black triangles in the thermal images indicate the position of the temperature sensor.

Vines were trained to vertical shoot positioning (VSP) in north-south-orientated rows with 1.8 m spacing between rows and 1.3 m vine spacing. Clusters of both cultivars (n = 6) were treated with a T_S set to 50 °C for 30 min with the lamp positioned 7 cm before the centre of the cluster where the sensor was placed, allowing sunlight to irradiate berries. Thermal and digital images of the berries were taken before and immediately after the lamps were switched off. The mean fruit surface temperature for each visible berry was calculated by the software. Berries (Silvaner: n = 135, Bacchus: n = 139) were classified as either symptomatic or non-symptomatic for SN by assessing the corresponding digital images for each thermal image.

3. Statistical analysis

R software (v. 4.0.3, R Core Team, 2020) was used to conduct statistical analysis. A simple linear regression was performed to predict the effect of calculated berry surface temperature on measured ΔFST. A Generalized Additive Model (Wood, 2011) was performed to predict the effect of measured berry surface temperature on measured electrolyte leakage.

To compare the susceptibility of both cultivars, odds ratios (OR) for developing symptoms of SN were calculated using a binary logistic regression model with 'Surface Temperature' and 'Cultivar' as predictors. The significance of both predictors was tested using the Wald Chi-Squared Test ($p < 0.05$). The Lethal Dose 50 (LD_{50}) for both cultivars was calculated using the function '*dose.p*' of the MASS package (Venables *et al*., 2002) with probability set to 0.5.

RESULTS

1. Influence of the distance of berry to heat source on berry hot spot temperature and received radiation

The initial FST_m of the heated berry was 21.6 °C before the lamp was switched on. As seen in Figure 3, the ΔFST increased to 8.6 °C at 20 cm distance and to 31.1 °C at 7 cm distance. ΔFST and the calculated E_b were strongly positively correlated (R^2 of 0.992 ($F(1,2) = 255$, $p < 0.004$). The ΔFST increased by 0.04 °C for each Wm^{-2} of calculated received radiation.

2. Comparison of actual berry temperature and Thermography

The T_A measured by the heating unit sensor reached the TS of 28 °C after nine minutes with a mean T_A value of 27.58 ± 0.08 °C until the end of the experiment. The temperature profile of the thermal camera measurements and thermocouple measurements of the berry surface followed a similar course after the steady state was reached at about 960 s, as shown in Figure 4. The temperature of the thermocouple sensors was 0.22 to 0.66 °C warmer at steady state compared to thermography measurements.

The FST_m measured by thermal imaging was 29.76 ± 2.90 °C and of thermocouple measurements was 29.33 ± 3.08 °C. There was no significant difference between both measurement techniques according to an independent-sample t-test ($t(125.5) = -0.81$, $p = 0.418$). Both measurements responded faster to the heat source and showed consistently higher temperature values (RMSE = 2.77 °C) compared to the heating unit sensor after a steady state was reached.

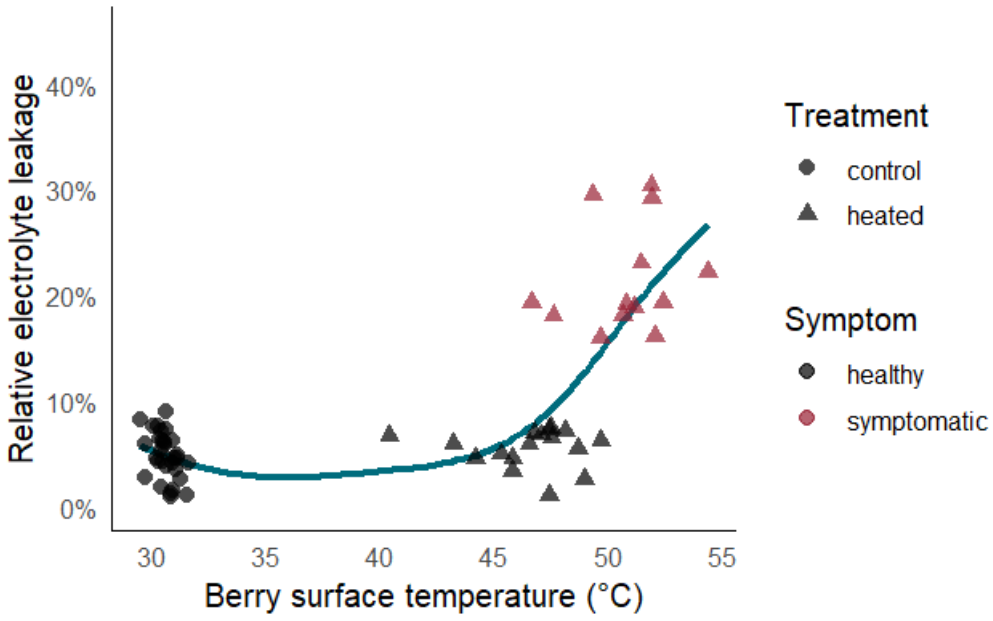

FIGURE 5. Electrolyte Leakage measurements.

Scatter plot of the measured relative electrolyte leakage against the surface temperature of berries that were either heated (triangle points) or at ambient conditions (control, filled circle). Red-coloured points indicate berries with symptoms of sunburn necrosis. The solid line represents a spline fit used to predict relative electrolyte leakage by berry surface temperature.

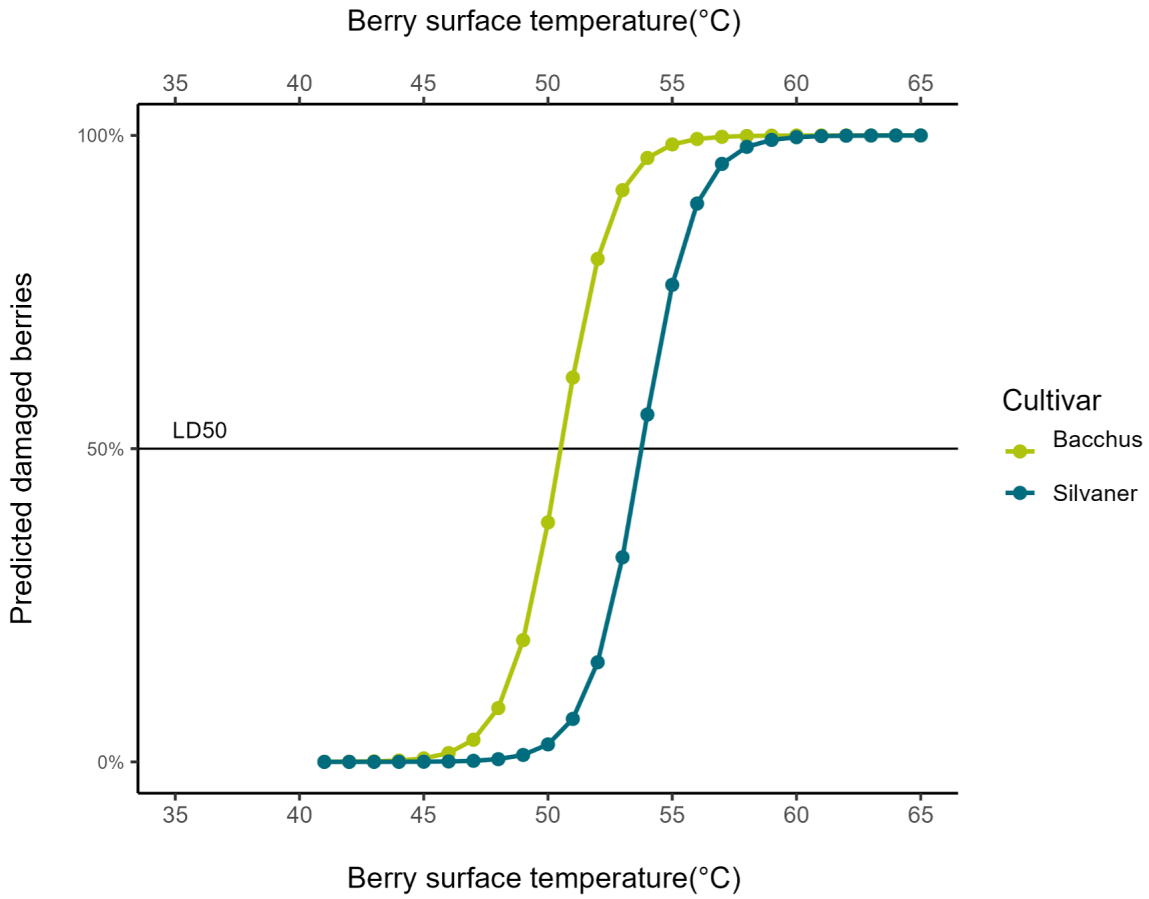

FIGURE 6. Prediction plot for sunburn necrosis symptoms on two cultivars.

Predicted probability of a berry showing symptoms of sunburn necrosis within 30 minutes of exposure to an altered berry surface temperature (°C) for cvs. Silvaner and Bacchus. The horizontal line indicates a probability of 50 % for a berry to be symptomatic (LD_{50}) within 30 minutes of high heat exposure.

3. Electrolyte Leakage Measurements

Figure 5 shows a scatter plot of measured REL against the FST of single berries (n = 60) that were either heated by the mobile device or at ambient temperatures (~ 30 °C), with sunlight being excluded during the heating. The mean REL of healthy control berries (n = 30) and healthy heated berries (n = 17) was 4.8 ± 0.4 % and 5.5 ± 0.4 %, respectively. The mean REL of symptomatic heated berries (n = 13) was at 21.5 ± 1.4 %. Symptomatic control berries were non-existent. A Generalized Additive Model was used to test the significance of the predictor '*berry surface temperature*' on '*relative electrolyte leakage*'. The regression model was significant ($R^2 = 0.63$, $F = 23.34$, $p < 0.001$), showing that higher FST led to higher REL in a non-linear relationship.

4. Comparing cv. Bacchus and Silvaner for sunburn susceptibility

A logistic regression model was used to predict the probability of berries having symptoms of SN using the predictors '*Surface Temperature*' (Wald = 83.30, p < .001) and '*Cultivar*' (Wald = 34.60, p < .001). An increase in temperature of 1 °C led to a 2.15 times higher chance of berries developing symptoms within 30 min of heating, represented by the slope of both prediction curves (Figure 6). A Lethal Dose (LD_{50}) was predicted based on the described model, showing that Bacchus approached LD_{50} at 50.51 ± 0.34 °C and Silvaner at 53.76 ± 0.35 °C, respectively. Comparing Bacchus and Silvaner, the odds for showing symptoms of SN were 14.49 times higher for Bacchus with every 1 °C increase in Surface Temperature, which is visualized as the shift in the prediction curve on the abscissa.

DISCUSSION

The device presented in this study was developed for the investigation of heat damage along a temperature profile between berries of individual clusters.

Adjusting the distance from berry to lamp has a major impact on ΔFST and can, therefore, be used to optimize the heating process. For certain research questions, natural sunlight on the fruit surface may be necessary during the heating process. Due to a cut-out on the upper visor of the spots, clusters were still exposed to sunlight when the sensor was at a 7 cm distance to the cluster, depending on the position of the sun. With a 7 cm distance, the calculated received radiation of a berry is approximately 620 Wm^{-2}, which would

correspond to a sunny day in summer, where global radiation varies between 600 and 1000 Wm^{-2}. Under indoor conditions (without solar radiation), this led to a ΔFST of 31.1 °C.

The heat energy applied to a berry decreases approximately by the squared distance to the heat source, enabling the establishment of temperature profiles within individual clusters. Altering the distance from berry to lamp can, therefore, be an effective way of achieving the desired berry temperatures depending on the experimental design and is easy to implement by the adjustable design of the heating unit construction. The positioning of the sensor and the lamp is therefore important for establishing the temperature profile along the cluster. Berries with a shorter distance to the lamp than the sensor will have higher temperatures as the chosen T_S and vice versa, since the power regulated by the control unit depends on the T_A provided by the heating sensor. During the heating process, berries reached somewhat higher temperatures than the chosen T_S (Figure 4). This systematic deviation is caused by the different physical properties of berries and sensors and is most likely linked to the water content of berries and the resulting enhanced capability of storing heat. As a result of the rather restrained temperature control algorithm, which decreases the power supply early before reaching T_S, the temperature was kept at a steady state after approx. 960 seconds. As the infrared lamps still emit heat after the power supply is turned down, the algorithm was programmed to carefully slow down the power supply when T_A approached T_S to avoid extreme overheating of the berries. A less restrained algorithm can be set anytime by changing the Python program to desired power values (%), depending on the experimental design.

The comparison of both fruit temperature measurement techniques shows that thermography may act as a more profound tool for monitoring FST compared to the use of thermocouples with the benefit of faster handling, the measurement of surfaces instead of single points and a non-destructive type of measurement. The variation within the thermocouple sensor measurements was greater in the first 10 minutes of heating compared to the infrared measurements, as indicated by their larger standard deviation in Figure 4. Additionally, the thermocouple sensors measured lower temperatures in the first 10 minutes of heating compared to the infrared measurements. Similar results have been obtained by Ranjan *et al*. (2020), who reported a close association of FST measured by thermal probe and thermography in apple fruit. As stated by Stoll and Jones (2007), the thermography of single berries on a cluster is much more effective compared to the usage of thermocouples. However, a continuous measurement during the heating process was not possible using thermography due to the radiation of the lamp that was reflected from the berry surface, leading to biased results, but could have been achieved using thermocouples.

Berries with visual symptoms of sunburn necrosis (e.g., brown-reddish colouring of skin and flesh) exhibit cell damage, expressed as an increase in REL. The higher REL of symptomatic berries compared to non-symptomatic and control berries indicates the well-known reaction of cell membranes to heat stress (Demidchik *et al*., 2014). In a comparable approach, Inaba and Crandall (1988) showed the non-linear relationship between fruit temperature and REL in tomato fruit. Our studies, however, reveal the large variation in FST required for symptoms to occur in grapevine berries. High and low values of REL were found for symptomatic and non-symptomatic berries in the range of ~ 46 to 50 °C. Non-symptomatic berries were not found at temperatures above 50 °C, and increased levels of REL were found exclusively on visually symptomatic berries, yielding a non-linear relationship between REL and FST. Additionally, these results indicate that a threshold temperature range with a rather large variation between single berries of a cluster exists for SN symptoms.

The threshold temperature for SN may vary significantly between cultivars. This was demonstrated by exposing clusters of cv. Bacchus, a cultivar that is well-known for its susceptibility to sunburn amongst growers to cv. Silvaner, which is considered to be a resilient cultivar, to the same heat load in the same timeframe. Berries of Bacchus showed SN symptoms at temperatures approximately 3 °C lower compared to Silvaner within the same timeframe. Similar temperatures were found for apples by Schrader *et al*. (2001), with ~ 52 °C and ten minutes required to induce SN symptoms. In this study, symptoms of SN on apples were observed with a delay of four days, while symptoms on berries in our study appeared after about 25–30 min of heat treatment. This facilitates the comparison of digital images and thermal images of the clusters to annotate symptomatic berries with corresponding fruit surface temperatures. As shown by REL measurements, berries without visual SN symptoms did not experience lethal cell damage.

The presented device is customizable at many levels. By adjusting T_S, the distance of the berry to the lamp, and the timeframe of heat applied, clusters can be set to a desired temperature profile. Each lamp can be controlled separately with a quick adjustment of height and distance to the cluster. The device is moveable within vineyards of common practice and may also be used in greenhouses or indoors. As heat stress response is studied in many fleshy fruits (Inaba and Crandall, 1988; Schrader *et al*., 2001; Yang *et al*., 2019), the device may also be adjusted to other crops that are cultivated in comparable cultivation systems like blueberries, tomatoes or apples.

CONCLUSION

The presented device allows the alteration of berry temperatures in a wide range of applications under field conditions. In combination with infrared thermography, the effects of controlled heat stress can be studied, yielding many replications with less dependency on weather conditions. This was demonstrated by estimating threshold temperatures for the occurrence of SN on berries for two cultivars. Therefore, it can be considered a useful tool for phenotyping for heat tolerance when reproducible conditions are required.

ACKNOWLEDGEMENTS

We thank the FDW (Forschungsring des deutschen Weinbaus) as well as the GFHG (Gesellschaft zur Förderung der Hochschule Geisenheim) for the financial support. Research in Washington was partly funded by the Washington State Grape and Wine Research Program and the Chateau Ste. Michelle Distinguished Professorship of Viticulture. We thank Dr. Markus Keller for his support in the implementation of the experiment in Washington. The authors acknowledge the great technical support provided by the Department of Agricultural Engineering (HGU) in constructing the device and validating the system. Mr. Klaus Konstantin Müller is acknowledged for his crucial help in designing and programming the temperature control unit.

REFERENCES

Demidchik, V., Straltsova, D., Medvedev, S. S., Pozhvanov, G. A., Sokolik, A., and Yurin, V. (2014). Stress-induced electrolyte leakage: the role of K+-permeable channels and involvement in programmed cell death and metabolic adjustment. *Journal of Experimental Botany* 65, 1259–1270. https://doi.org/10.1093/jxb/eru004

Gambetta, J. M., Holzapfel, B. P., Stoll, M., and Friedel, M. (2021). Sunburn in Grapes: A Review. *Front. Plant Sci.* 11, 604691. https://doi.org/10.3389/fpls.2020.604691

Gill, S. S., and Tuteja, N. (2010). Reactive oxygen species and antioxidant machinery in abiotic stress tolerance in crop plants. *Plant Physiology and Biochemistry* 48, 909–930. https://doi.org/10.1016/j.plaphy.2010.08.016

Gouot, J. C., Smith, J. P., Holzapfel, B. P., and Barril, C. (2019). Impact of short temperature exposure of *Vitis vinifera* L. cv. Shiraz grapevine bunches on berry development, primary metabolism and tannin accumulation. *Environmental and Experimental Botany* 168, 103866. https://doi.org/10.1016/j.envexpbot.2019.103866

Hulands, S., Greer, D. H., and Harper, J. D. I. (2014). The Interactive Effects of Temperature and Light Intensity on *Vitis vinifera* cv. 'Semillon' Grapevines. II. Berry Ripening and Susceptibility to Sunburn at Harvest. *Europ.J.Hort.Sci* 79, 1–7.

Inaba, M., and Crandall, P. G. (1988). Electrolyte Leakage as an Indicator of High-temperature Injury to Harvested Mature Green Tomatoes. *J. Amer. Soc. Hort. Sci.* 113, 96–99. https://doi.org/10.21273/JASHS.113.1.96

IPCC, Masson-Delmotte, V., Zhai, P., Pirani, A., Connors, S. L., Péan, C., et al. (2021). Climate Change 2021: The Physical Science Basis. Contribution of Working Group I to the Sixth Assessment Report of the Intergovernmental Panel on Climate Change. *Cambridge University Press*, 2391. https://doi.org/10.1017/9781009157896

Kolb, C. A., Wirth, E., Kaiser, W. M., Meister, A., Riederer, M., and Pfündel, E. E. (2006). Noninvasive Evaluation of the Degree of Ripeness in Grape Berries (*Vitis vinifera* L. Cv. Bacchus and Silvaner) by Chlorophyll Fluorescence. *J. Agric. Food Chem.* 54, 299–305. https://doi.org/10.1021/jf052128b

Meehl, G. A., and Tebaldi, C. (2004). More Intense, More Frequent, and Longer Lasting Heat Waves in the 21st Century. *Science* 305, 994–997. https://doi.org/10.1126/science.1098704

Modest, M. (2003). *Radiative Heat Transfer*. 2. Elsevier https://doi.org/10.1016/B978-0-12-503163-9.X5000-0

Munné-Bosch, S., and Vincent, C. (2019). Physiological Mechanisms Underlying Fruit Sunburn. *Critical Reviews in Plant Sciences* 38, 140–157. https://doi.org/10.1080/07352689.2019.1613320

PEWA, M. G. ed. (2009). Leitfaden zur Infrarot-Messtechnik. Available at: www.pewa.de [Accessed July 14, 2021].

R Core Team (2020). R: A language and environment for statistical computing. Available at: https://www.R-project.org/

Ranjan, R., Khot, L. R., Peters, R. T., Salazar-Gutierrez, M. R., and Shi, G. (2020). In-field crop physiology sensing aided real-time apple fruit surface temperature monitoring for sunburn prediction. *Computers and Electronics in Agriculture* 175, 105558. https://doi.org/10.1016/j.compag.2020.105558

Sadras, V. O., Montoro, A., Moran, M. A., and Aphalo, P. J. (2012). Elevated temperature altered the reaction norms of stomatal conductance in field-grown grapevine. *Agricultural and Forest Meteorology* 165, 35–42. https://doi.org/10.1016/j.agrformet.2012.06.005

Schrader, L. E., Zhang, J., and Duplaga, W. K. (2001). Two Types of Sunburn in Apple Caused by High Fruit Surface (Peel) Temperature. *Plant Health Progress* 2, 3. https://doi.org/10.1094/PHP-2001-1004-01-RS

Spayd, S. E., Tarara, J. M., Mee, D. L., and Ferguson, J. C. (2002). Separation of Sunlight and Temperature Effects on the Composition of *Vitis vinifera* cv. Merlot Berries. *Am J Enol Vitic.* 53, 171–182. https://doi.org/10.5344/ajev.2002.53.3.171

Stoll, M., and Jones, H. G. (2007). Thermal imaging as a viable tool for monitoring plant stress. *OENO One* 41, 77. https://doi.org/10.20870/oeno-one.2007.41.2.851

Tarara, J. M., Ferguson, J. C., and Spayd, S. E. (2000). A Chamber-Free Method of Heating and Cooling Grape Clusters in the Vineyard. *Am J Enol Vitic.* 51, 182. https://doi.org/10.5344/ajev.2000.51.2.182

Venables, W. N., Ripley, B. D., and Venables, W. N. (2002). *Modern applied statistics with S*. 4th ed. New York: Springer.

Venios, X., Korkas, E., Nisiotou, A., and Banilas, G. (2020). Grapevine Responses to Heat Stress and Global Warming. *Plants* 9, 1754. https://doi.org/10.3390/plants9121754

Wahid, A., Gelani, S., Ashraf, M., and Foolad, M. (2007). Heat tolerance in plants: An overview. *Environmental and Experimental Botany* 61, 199–223. https://doi.org/10.1016/j.envexpbot.2007.05.011

Wood, S. N. (2011). Fast Stable Restricted Maximum Likelihood and Marginal Likelihood Estimation of Semiparametric Generalized Linear Models. *Journal of the Royal Statistical Society Series B: Statistical Methodology* 73, 3–36. https://doi.org/10.1111/j.1467-9868.2010.00749.x

Yang, F.-H., Bryla, D. R., and Strik, B. C. (2019). Critical Temperatures and Heating Times for Fruit Damage in Northern Highbush Blueberry. *horts* 54, 2231–2239. https://doi.org/10.21273/HORTSCI14427-19